

# Notes on results for the new flux of Vishniac in a galactic dynamo model with turbulent velocity increasing with distance from midplane.

August 17, 2024

## 1 Introduction

Refer to the old 2012 draft “nvf.pdf” for more details. Here we use the same code. The main difference is that instead of assuming the turbulent velocity to be constant and the density profile stratified with

$$\rho \propto \exp(-z^2/h^2) \quad (\text{old model})$$

we now assume the turbulent velocity to be stratified according to

$$u = u_0 \exp\left(\frac{z^2}{2h^2}\right), \quad (1)$$

with the density  $\rho$  constant. As with the old model we also take the correlation time  $\tau$  constant. Then the turbulent diffusivity

$$\eta_t = \frac{1}{3}\tau u^2 = \frac{1}{3}\tau u_0^2 \exp\left(\frac{z^2}{h^2}\right), \quad (2)$$

and the equipartition field strength is given by

$$B_{\text{eq}} = 4\pi\rho u^2 = 4\pi\rho u_0^2 \exp\left(\frac{z^2}{h^2}\right) = B_0 \exp\left(\frac{z^2}{h^2}\right). \quad (3)$$

We also try an alternative model where  $B_{\text{eq}} = \text{const}$  which implies  $\rho \propto \exp(-z^2/h^2)$ .

## 2 New flux term (from “nvf.pdf”)

The new flux density of mean small-scale magnetic helicity density of Vishniac is given by

$$\mathcal{F}^{NV} = -\frac{\omega\tau_c^2 b^2}{3} \left[ \left( \frac{2}{5} + \frac{11}{15}q \right) u^2 + \frac{13}{66}q \frac{b^2}{4\pi\rho} \right] \hat{z}, \quad (4)$$

where  $b$  is the rms value of the fluctuating part of the magnetic field,  $\omega\hat{z}$  is the angular velocity and  $q \equiv -d\ln\omega/d\ln r$ . Defining  $\xi \equiv b^2/B_{\text{eq}}^2$ , we find

$$\mathcal{F}^{NV} = -4\pi\omega\rho\eta_t^2\xi \left( \frac{6}{5} + \frac{11}{5}q + \frac{13}{22}q\xi \right) \hat{z} = -16\pi f\omega\rho\eta_t^2\hat{z}, \quad (5)$$

where use has been made of Eq. (2), and where

$$f(q, \xi) \equiv \frac{\xi}{4} \left( \frac{6}{5} + \frac{11}{5}q + \frac{13}{22}q\xi \right).$$

Reasonable values for galaxies are  $q = 1$  and  $0.1 < \xi < 1$ ;  $f(1, 1) \simeq 1$  and  $f(1, 0.1) \simeq 0.09$ .

Table 1: List of models.

Model	$R_\omega$	$R_\alpha$	$R_U$	$R_\kappa$	$f$	$u$	$\rho$
A	-20	0	0	0	1	$\propto \exp[z^2/(2h^2)]$	const
B	-20	0	0.45	0	1	$\propto \exp[z^2/(2h^2)]$	const
C	-20	0	0.45	0	1	$\propto \exp[z^2/(2h^2)]$	$\propto \exp[-z^2/h^2]$
D	-20	0	0.45	0	0.1	$\propto \exp[z^2/(2h^2)]$	const

### 3 Relation to Sharanya’s notes

Recall that Sharanya had made the first notes on this effect in galaxies, but without having at his disposal the “latest” detailed expression for the flux, i.e. expression (5), and also without knowing the correct sign of the flux. He tried both positive and negative signs. He chose to make  $u \propto \exp[-z^2/(2h^2)]$ . All or at least most of his results were reproduced precisely using my 1D code, as I recall. He found that by choosing one sign for the flux, a saturated steady state with  $B \sim B_{\text{eq}}$  can be reached, while for the other sign, one also gets a saturated state with  $B \sim B_{\text{eq}}$  but with oscillations (it’s not clear to me from his notes which sign corresponds to which result).

Now the direction chosen for the stratification relevant for the divergence of the flux was the same as Sharanya’s choice in our old model of “nvf.pdf” (though we took  $\rho$  rather than  $u$  to be stratified, as explained above), but the direction of the divergence of the flux is different in this new model. In “nvf.pdf” we found oscillating near-equipartition solutions as Sharanya had found for a certain sign of the flux. So given Sharanya’s results we would expect that with our new model we should find steady near-equipartition solutions, since the divergence will now have the opposite sign.

## 4 Results

We use the same 1D mean-field galactic dynamo code as used for “nvf.pdf.” The only important differences are those mentioned in Sec. 1 above. My newer codes improve on this old code, but do not yet include the new flux, so for now I decided to stick with the old one for convenience and consistency. (But a next step would be to switch to the new code which is faster and better organized, and contains a few additional features.) As we are mainly interested in steady solutions, I have done the new runs assuming FOSA rather than MTA, because MTA is unlikely to be important for solutions that are not oscillating. Models are shown in Table 1. Figures are plotted in computational units. Velocity units are such that  $1 \text{ km s}^{-1} = 1.5$  computational units if typical values are assumed for physical parameters like  $u = 10 \text{ km s}^{-1}$  at the midplane and  $h = 0.5 \text{ kpc}$ .

### 4.1 Model A

Clearly  $\alpha_m$  builds up to unreasonably large values at the boundaries. Thus, an additional flux of  $\alpha_m$  is required, such as the advective flux in the presence of an outflow. The time evolution shows that the solution is not very stable. Due to the boundary layers of  $\alpha_m$ , these results cannot be considered to be realistic.

### 4.2 Model B

Now a modest outflow has been assumed to be present. The vertical outflow velocity is zero at the midplane but increases linearly to 0.45 at the disk boundaries. The boundary layer of  $\alpha_m$  is reduced in magnitude, and  $\alpha_m$  is now comparable to  $u$ , (not significantly greater than  $u$  which might be unreasonable). The solution is quadrupolar and steady, with magnitude of the magnetic pitch angle peaking toward the disk boundaries. Model B acts as the fiducial model. I checked that if the stratification is inverted, so that the sign of the flux changes, we do indeed recover a growing oscillating quadrupolar solution that saturates near equipartition but still oscillates.

### 4.3 Model C

Here we take the parameters of Model B except that now  $B_{\text{eq}} = \text{const}$  which means that  $\rho \propto u^{-2}$ . Results are very similar to those of Model B. Similarly, if we make the outflow velocity equal to zero, then we get results very similar to Model A.

### 4.4 Model D

Here we take  $f = 0.1$ , which is perhaps more realistic than  $f = 1$ . For a flat rotation curve this corresponds to  $\xi = 0.12$ . The results resemble qualitatively those of Model B. The saturated field and kinematic growth rate are smaller than those in Model B.

## 5 Discussion

The effect seems to work as expected. The turbulent velocity profile chosen is quite reasonable, and probably more reasonable than what was assumed in our previous attempts that showed oscillating solutions for the correct sign of the flux. As shown in “nvf.pdf” oscillating solutions would lead to radial reversals every  $\sim h$ . Although at least one large-scale reversal may be present in our Galaxy, observations of other galaxies favour large-scale fields that do not have reversals. Therefore, it seems likely that such oscillating solutions are not prevalent in nature. Our new results show that when probably the most likely sign of the stratification is assumed, we indeed get growing and then saturating steady near-equipartition quadrupole solutions, so long as  $\alpha_m$  can be advected outward at the boundary. This is true even for  $\xi = b^2/u^2$  as small as 0.1.

## 6 Conclusion

This effect looks even more promising with these new results because it can probably explain the presence of steady quadrupolar near-equipartition large-scale fields seen in galaxies.

## 7 Further questions

Here are some outstanding questions:

- Under what conditions does this effect dominate over the standard kinetic  $\alpha$ -driving, and what happens when both effects are included?
- Will a diffusive rather than advective flux of  $\alpha_m$  be sufficient to avoid the boundary layers?
- How do the predictions of this model, for example pitch angle, growth rate, compare with predictions of more standard  $\alpha\Omega$  dynamo models?
- How would the results be affected by taking into account tangling of the LS field to produced SS field, making  $\xi$  a dynamical quantity?
- How should this mechanism be understood physically?
- Can we write down an analytical solution (e.g. no- $z$ )?
- Etc.

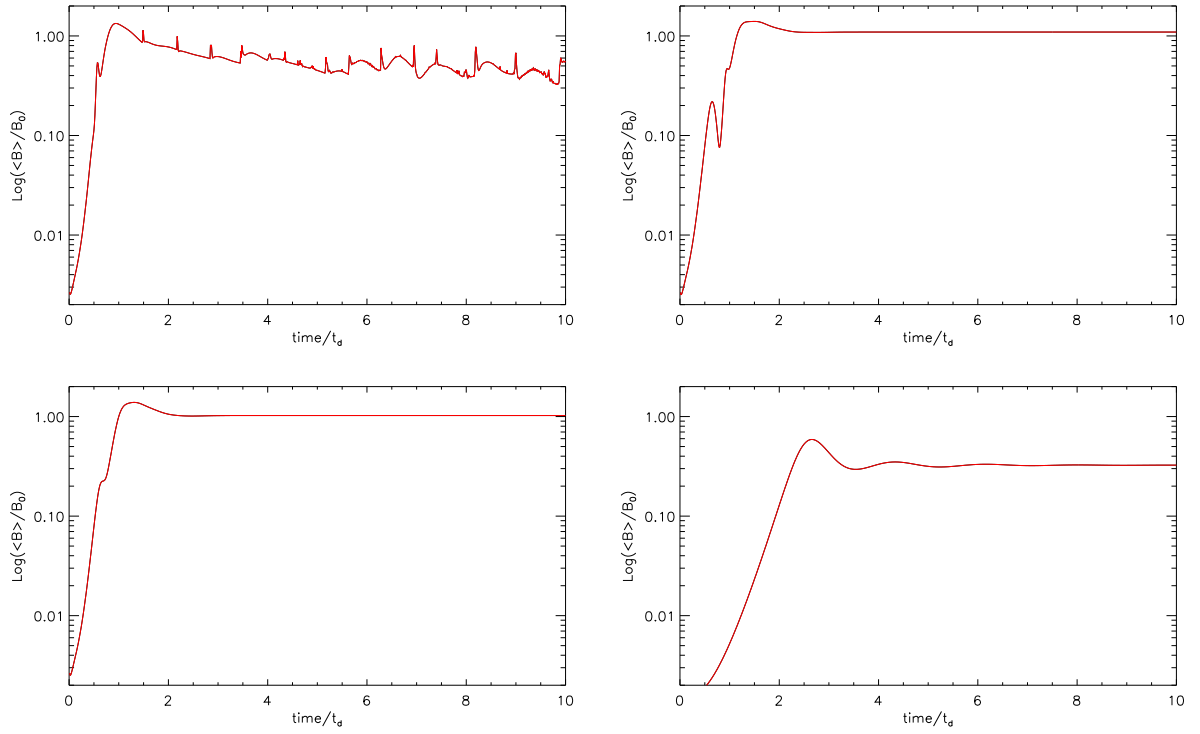


Figure 1: Time evolution for the different models: A (top-left), B (top-right), C (bottom-left), D (bottom-right). Note that Model A was evolved up to  $t = 30$  but did not show qualitatively different behaviour. Here  $t_d = h^2/\eta_t|_{z=0}$ ,  $B_0 = B_{\text{eq}}(0)$  and field values are rms spatial averages across the disk.

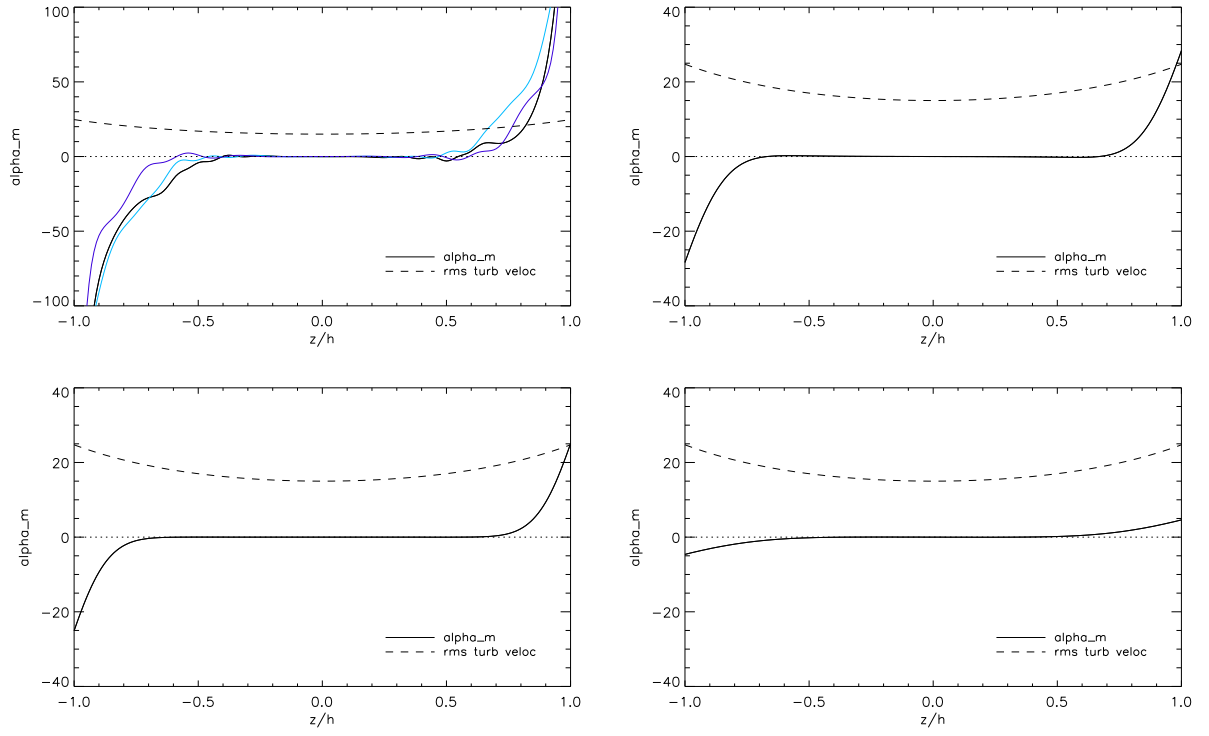


Figure 2: Similar to Fig. 1 but now showing  $\alpha_m$  with respect to  $z/h$ . For Model A colours represent times: 2.5, 5 and 10  $t_d$ . The rms turbulent speed is shown with a dashed line for reference. Note the different range for the Model A plot.

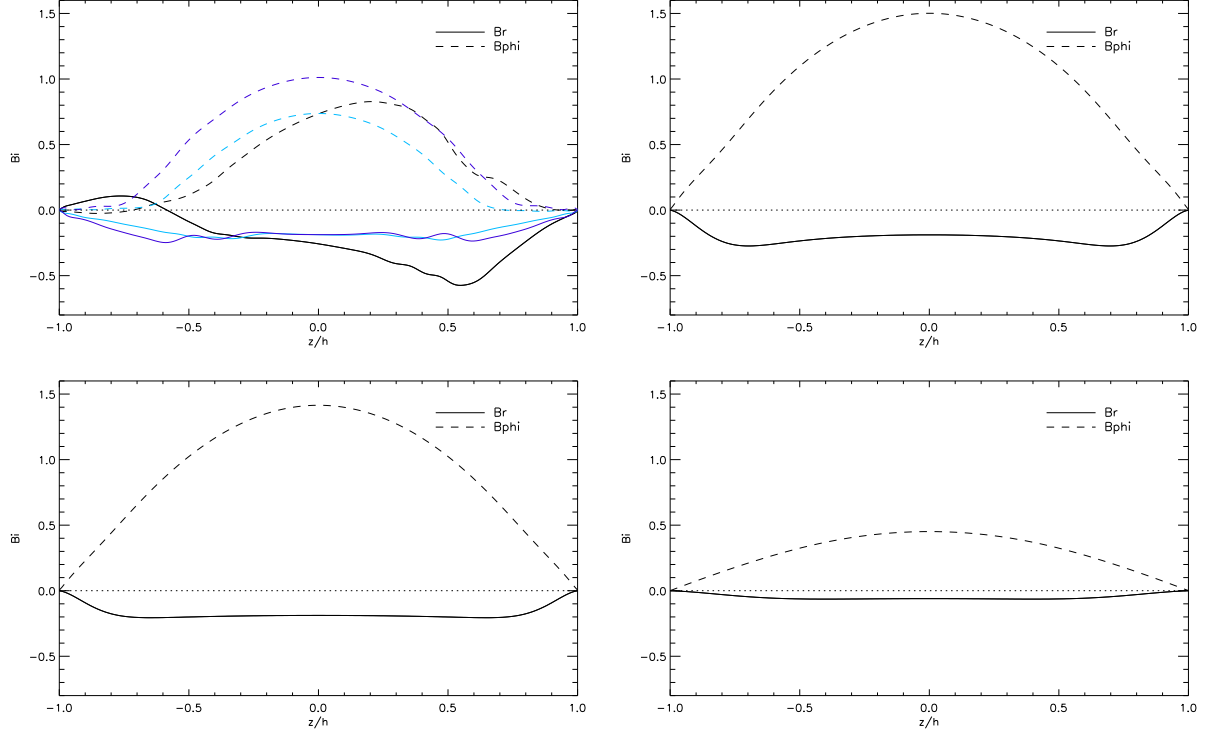


Figure 3: Similar to Fig. 2 but now showing  $B_r(z)$  and  $B_\phi(z)$  at  $t = 10t_d$ .

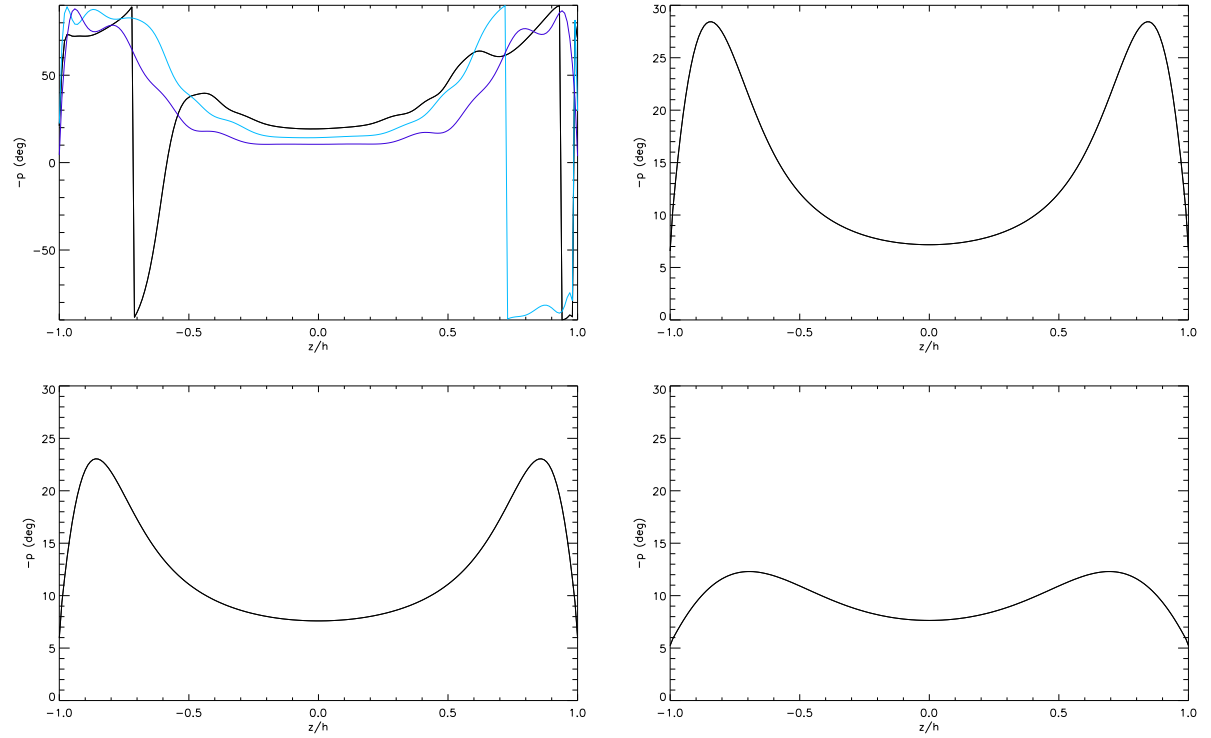


Figure 4: Similar to Fig. 2 but now showing magnetic pitch angle  $-p(z)$  at  $t = 10t_d$ . Note the different range for the Model A plot.